Research Article

Thermodynamic assessment of human feces gasification: an experimental-based approach

Flávio Lopes Francisco Bittencourt[1,2] · Atílio Barbosa Lourenço[2] · Elias Antônio Dalvi[2] · Márcio Ferreira Martins[2]

Abstract
Residues with a large amount of organic content represent a potential for energy recovery. Specifically human feces, given the amount of global production and the environmental appeal, appear as a potential candidate for a new feedstock. The objective of this work is to perform a thermodynamic assessment of human feces gasification considering for the first time all inefficiencies of a downdraft gasifier. A thermochemical characterization was conducted from the sterilized raw material to the products. New data and discussions about the conversion efficiencies for such type of fuel are brought up, such as the influence of the exothermic pyrolysis on the chemical exergy destruction. The results suggest an unfavorable application in energetic terms; however, when the exergy analysis is added with the environmental bias, the process becomes more attractive due to the high physical exergy.

Keywords Human feces · Exothermic pyrolysis · Gasification · Syngas · Exergy

1 Introduction

Thermochemical conversion of biomass (e.g., sugarcane bagasse, coconut shell, rice husk, banana leaves, etc.) has been a field of interest since the last decades [1–4], and now a variety of solid fuels are categorized in terms of chemical, physical, thermochemical and thermodynamic properties. On the other hand, the solid residues such as the sewage and algal sludges residues from water treatment plants, and raw human feces appear in the scenario of conversion technologies in need of characterization. These solids have a relatively large amount of organic content soaked in water, more than 75%. Even though the organic content may confer to them a biomass characteristic, the biosolids classification seems to be more appropriated [5]. However, to use these residues as an energy source, reducing the water content to the level required for thermochemical conversion technologies is still a challenge. Very few works have attempted to convert human feces [5–8], and the conversion has been reached by mixing feces with inert materials, e.g., sand [5], or with plastic materials [8]. Heretofore, the only successful case of converting raw feces has been made in a bench-scale fixed bed reactor [6].

Some authors explored the thermochemical characterization of simulated feces on smoldering combustion [9–11], and gasification [6, 12], but to reproduce feces is a very complex challenge considering its heterogeneous characteristics. Nevertheless, the results were very encouraging. Monhol and Martins [8] conducted combustion of real feces, showing that a high energy content could be recovered. Recently, Jurado et al. [13] developed preliminary work on a micro-combustor prototype to recovery energy from human feces. Tests were carried on surrogate feces and then applied on real feces. Yacob et al. [14] performed slow pyrolysis experiments on human feces, quantifying the char yield and gas evolution. Yet, some contradictory results are found in the literature. For instance, Onabanjo et al. [12] reported for real feces an average amount of 51% of ash, 17% of volatile matter and

✉ Márcio Ferreira Martins, marcio.martins@ufes.br | [1]Federal Institute of Espirito Santo, 660 Augusto Costa de Oliveira St., Piuma, Brazil. [2]Laboratory of Combustion and Combustible Matter, Federal University of Espirito Santo, 514 Fernando Ferrari Av., Vitoria, Brazil.

SN Applied Sciences (2019) 1:1077 | https://doi.org/10.1007/s42452-019-1104-1

Received: 17 June 2019 / Accepted: 16 August 2019 / Published online: 23 August 2019

32% of fixed carbon, and for simulant feces an average amount of 14% of ash, 86% of volatile and 0% of fixed carbon, both analysis on dry basis. Jurado et. al [13] reported no presence of fixed carbon neither for real nor simulant feces. Although these previous studies delivered large contributions in the field of waste management, it did not account for a detailed thermochemical characterization of real human feces as a solid fuel. Here, for the first time, the exothermic characteristic of human feces pyrolysis is experimentally presented. According to Roberts [15], the exothermic pyrolysis can release around 8–10% of the heat content of the feedstock. A few works show experimental evidence on this subject [16]; however, the exothermic behavior is only revealed when separating the main constituents of wood—hemicellulose, cellulose and lignin.

Since the conversion of human feces is not fully understood and there is no conversion technology developed for such potential fuel, the gasification technology is still a good reference, even though it has been built for wood biomass. To suggest gasification as one way to recover energy from feces, a thermodynamic analysis is more suitable. The method of exergy analysis is an engineering tool applied to assess the performance of energy conversion processes and systems in light of the second law of thermodynamics. Exergy is defined as the maximum theoretical potential of a system energy amount that can be converted in work, regarding a reference environment [17]. Such potential can be split into two fractions, namely physical exergy and chemical exergy. Physical exergy is the work potential fraction due to pressure and/or temperature difference of the system and environment, while chemical exergy is the remaining fraction due to composition difference. Then, exergy may be interpreted as an indicator that put all energy quantities on the same basis for comparison, i.e., their respective potentials to do work. As exergy is destroyed along processes due to irreversibilities, instead of being conserved as energy is, the true thermodynamic inefficiencies of processes are revealed [18].

Several exergy analyses of gasification process have been done and related in the literature. Ptasinski et al. [19] performed a comparative study for the gasification exergy efficiency of different types of biofuels (wood, vegetable oil, sludge and manure) and benchmarked it against the gasification of coal. Pellegrini and De Oliveira [20] and Onabanjo et al. [12] performed an exergy analysis of sugarcane bagasse and human feces gasification, respectively. All these works were conducted under theoretical assumptions, applying a thermodynamic equilibrium model with an adiabatic reactor. As previously established by Gomez and Leckner [21] and Arnavat et al. [22], the equilibrium model overestimates the production of H_2 and CO, underestimates CO_2 and almost zero out the concentration of CH_4, tars and char.

At present, the suitability of human feces as a feedstock for gasification is exclusively based on theoretical assumptions that occasionally lead to unrepresentative descriptions of the actual process. In this work, a thermodynamic assessment of human feces gasification is performed considering for the first time the inefficiencies of a downdraft gasifier. Thus, the real state of the thermochemical conversion of such residue is achieved for an existent technology. The thermochemical characterization from the sterilized material to the products streams is also presented.

2 Materials and methods

2.1 Raw material

The raw feces used in experiments were collected directly from the dry sanitary toilets installed at the Laboratory of Combustion and Combustible Matter from the Federal University of Espirito Santo, Brazil. Notable characteristics were strong odor and dark coloration. For security and hygiene procedures, the raw feces were sterilized inside ovens at 105 °C, to prevent proliferation and action of pathogens. Later, an open-air drying treatment followed by mass measurements was conducted to leave the material with three moisture contents: 0%, 10% and 20% which according to the literature is the maximum acceptable value to conduct experiments in a downdraft gasifier [23].

2.2 Experimental device and protocol

Thermal analyses were performed using TA INSTRUMENTS model SDT Q600, where both thermogravimetric and differential thermogravimetric analyses were performed simultaneously. The samples were prepared with 3.0 mg, and the heating rate was set on 10 °C/min up to 600 °C, whereas the flow rate of atmosphere gas was fixed at 100 mL/min. The experiments were repeated with an inert atmosphere (N_2) and oxidative (air) atmosphere. A non-standard proximate analysis combining TG and DSC was used to determine the fractions of fixed carbon, volatile matter and ash.

Inductively coupled plasma optical emission spectrometry (ICP OES) was used for chemical characterization, following standard ASTM 5373-93. Levels of carbon, hydrogen, phosphor and sulfur were also set. Nitrogen levels were determined by the method Kjeldahl 4500-Norg. The amount of ash was determined following Standard ASTM 3174-00.

Batch gasification process was conducted on the downdraft Biomass Gasifier ALL POWER PELLET GEK 20 kW. The full description of the device and gasification protocol can be referred in [24]. The gasifier was fed at the top with 300

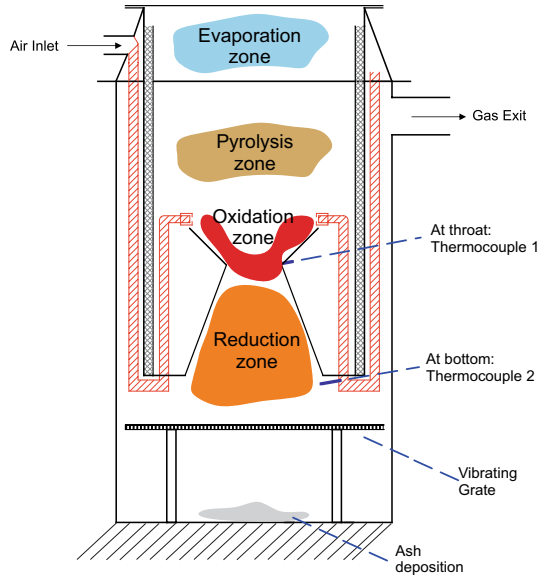

Fig. 1 Experimental device used for batch gasification

Table 1 Parameters for batch gasification of sterilized human feces

Parameter of gasification	Value
Moisture (%)	0, 10 and 20
Mass (kg)	0.300
Air flow rate (L/s)	0.291
Operating pressure (kPa)	99.96
Temperature (°C)	25

g of the feedstock, following the zones of drying, pyrolysis, oxidation and reduction. The heat generated from the reaction char + O_2 (oxidation zone) was responsible for providing conditions for pyrolysis and for drying the feces in the other zones. Since a downward flow was established, tar was cracked within the reduction zone, leaving the output gas tar-free. The airflow rate was fixed at 0.291 L/min and the pressure was 99.96 kPa. The temperature was monitored through the whole process by thermocouples located at the throat and the bottom, as shown in Fig. 1.

Gases produced were directed to the flare, while a part was conducted through a silicone hose connected to the gas analyzer TESTO 454 M/XL, capable of performing online measuring. When the flare was active, it was an indication that combustible gases were being produced. Before entering the analyzer, the gases passed through an intermediate dry filter to prevent penetration of particulates. The experiments were repeated for the three moisture samples to check the influence on the thermochemical conversion. Table 1 summarizes the parameters of gasification.

2.3 Thermodynamic methodology

The classical approach presented in Kotas [18] is followed, where a mass, energy and exergy balance are given in detail and well explained. The computer software Engineering Equation Solver [25] was used to implement and perform the calculations. As the gasification is a batch process, 0.3 kg of fecal material and moisture values of 0%, 10% and 20% were used as an input for the analysis. Due to the local environmental conditions, the input air for the model was a binary mixture of N_2 and O_2 in wet conditions (80% of water at 99.96 kPa, Table 1). The equations that model the problem will be presented along with the results section, already including the experimental-based approach, i.e., feces characterization and the gasifier's measurements. The thermodynamic methodology can be summarized into the three steps as follows:

- A mass balance is performed using data from the ultimate analysis, non-standard proximate analysis and from the syngas composition to balance the chemical equations.
- The molar composition and the temperature of the syngas for each moisture content are used to perform the energy balance. Here, key parameters as the cold gas efficiency (CGE) and heating value are determined, also using data from the proximate and ultimate analysis.
- At last, the exergy balance is performed to identify and quantify the inefficiencies related to the gasification process, using the results from mass and energy balance.

3 Results and discussion

3.1 Analysis of sterilized feces

3.1.1 Thermogravimetric analysis (TGA) and differential scanning calorimetry analysis (DSC)

From 30 to 150 °C, TGA under air (Fig. 2a) reveals two peaks of mass loss, representing around 17.3%. The first one is around 50 °C and can be related to the release of some volatile organic compounds (VOCs) typically found in feces, such as ethanoic, butanoic, pentanoic acids, benzaldehyde, ethanal, carbon disulfide, dimethyl disulfide, acetone, 2-butanone, 2, 3-butanedione, 6-methyl-5-hepten-2-one, indole and 4-methylphenol [26, 27]. The second peak, around 80 °C, can be related to water evaporation. Both are characterized by an endothermic valley on DSC under air (Fig. 2c). From 150 to 400 °C, approximately 50.2% of mass loss is observed. This mass loss is related to the major breakdown mechanism in feces: the overlap

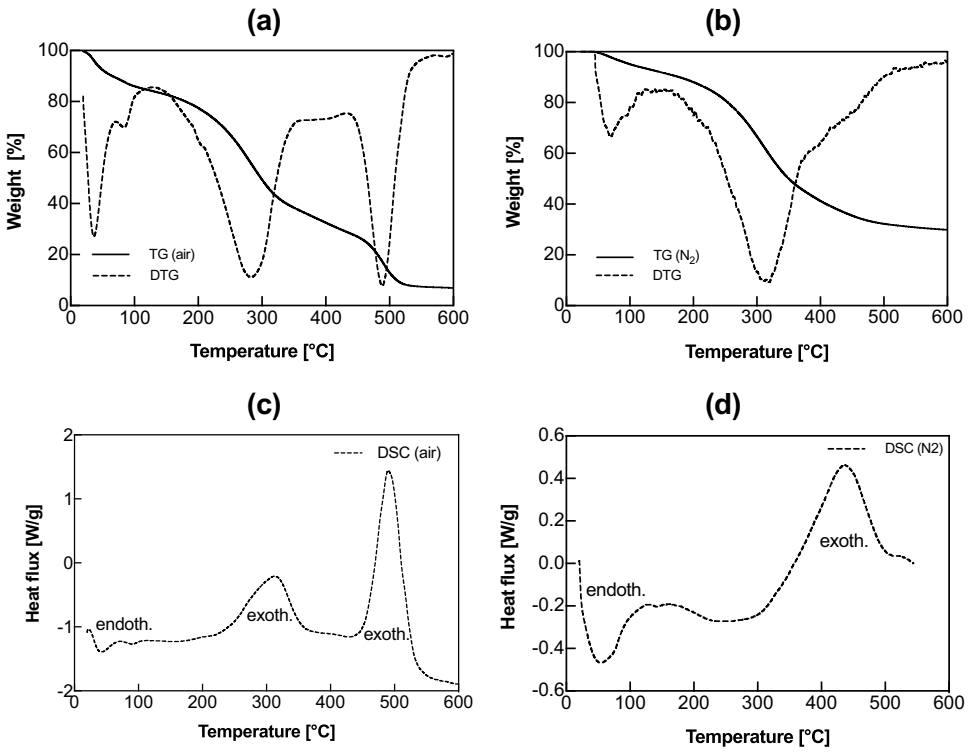

Fig. 2 Thermal analysis of human feces: **a** TG/DTG under air, **b** TG/DTG under N_2, **c** DSC under air, and **d** DSC under N_2. Heating rate at 10 °C/min

pyrolysis and homogeneous/heterogeneous reactions. Between this temperature range, DSC (Fig. 2c) shows only one exothermic peak, characterizing that the energy released is an average positive value from all reactions. Noteworthy, there is no consensus in the context of solid combustion, about the real contribution of the gas phase oxidation on the heat release [28, 29]. This issue will not be addressed in this work. From 400 to 550 °C, almost 25.1% of mass loss is observed. This loss is related to the oxidation of char, confirmed by DSC, where a strong exothermic peak is noted. Furthermore, no mass loss was observed, remaining 7.4% of ash.

We now call the attention for pyrolysis, represented in Fig. 2b (TG/DTG) and Fig. 2d (DSC). From 30 to 150 °C, following the same fashion of TG under air, a mass loss related to water evaporation and volatiles release is observed, while DSC also reveals only one and wide endothermic valley. From 150 to 500 °C almost 60% of mass loss occurs. As a first guess, it is related to overall pyrolysis forming char. Combining the remaining mass on both TG under air (about 7%) and TG under N_2 (about 32%), the char amount is about 25%. Table 2 shows the proximate, ultimate analysis and ash composition of human feces and other solid fuels.

Concerning Fig. 2d, a strong exothermic peak is observed. However, pyrolysis generally is noted for presenting endothermic reactions, since devolatilization normally consumes energy. The fact is that a large amount of the VOCs have oxygen on composition and as the compounds get released, these oxygen molecules turn the atmosphere oxidative. It is important to state that the DSC curve shows the overall balance of energy, meaning that during this stage, exothermic reactions released more energy than endothermic reactions from devolatilization consumed, characterizing the exothermicity of pyrolysis. Nevertheless, the exothermic energy and the oxygen released provided conditions only for partial char oxidation. Yang et al. [16] also observed an exothermic behavior during cellulose pyrolysis for temperatures above 400 °C, trying to explain the competition between endothermic and exothermic reactions in wood pyrolysis.

To ascertain the result found, we also conducted DSC under N_2 (Fig. 3) for chicken and pig feces. It is observed the same behavior of human feces, highlighting the

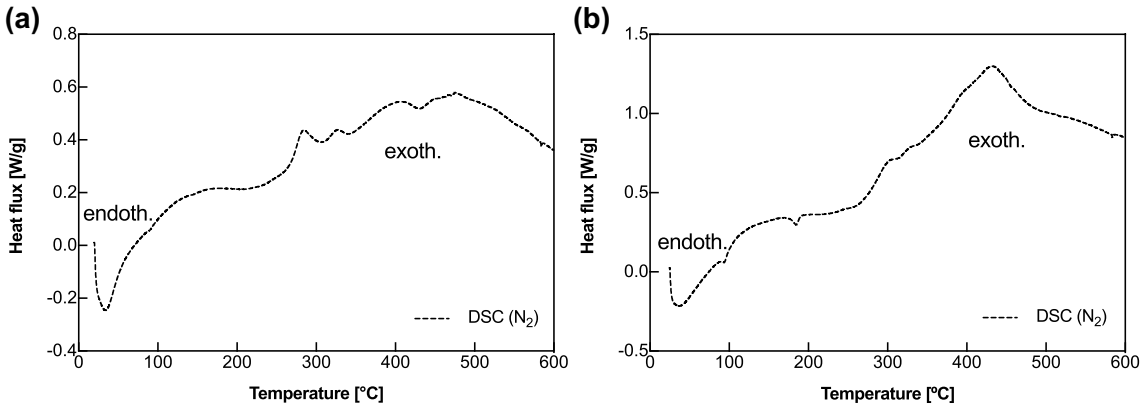

Fig. 3 DSC under N_2 from **a** chicken and **b** pig feces, both presenting exothermic peaks during pyrolysis. Heating rate at 10 °C/min

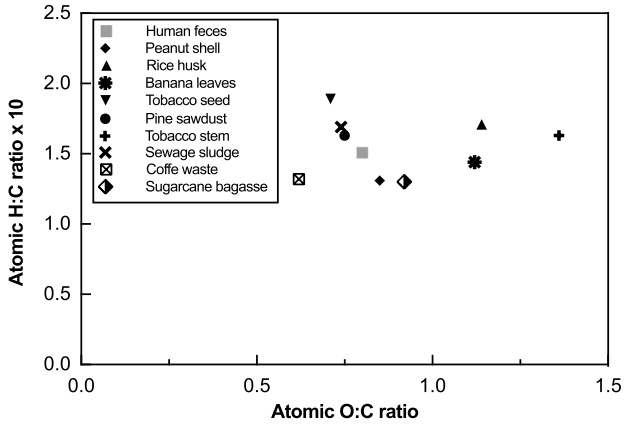

Fig. 4 Van Krevelen chart for human feces (gray) and other solid fuels (black). Data from [1, 2, 32, 51, 53, 54, 56, 57]

influence of VOC during pyrolysis. After 200 °C, an exothermic peak is dominant in both analysis, ratifying our previous observation.

By integrating DSC curves in time, it was possible to obtain the heat of reaction by the mass of samples for each peak. Performing a simple energy balance, the evaporation energy demand (210.5 J/g) could be covered by the exothermic pyrolysis energy (545.5 J/g), leading to a positive balance (335 J/g) of the overall pyrolysis process. It means that theoretically, for a chemical kinetics dominant phenomenon there is a given level of moisture that could be dried using the energy from pyrolysis (from 8 to 10% according to Roberts [15]). In terms of combustion, the overlapped pyrolysis and homogeneous/heterogeneous reactions had a positive heat of reaction of 865 J/g, while char oxidation reached 1562 J/g of sample.

3.1.2 Chemical characterization

Table 2 also shows the chemical composition of feces, trying to establish some comparison with categorized biomass. Also, biosolids are included since such residue has an important amount of organic matter, with a similar composition to human feces in terms of proximate and ultimate analysis. A few authors refer to human fecal material as a categorized biomass [6, 12, 14, 30], but the high levels of moisture content tend to approximate their classification as a biosolid. Indeed, while eliminating the water levels, the biomass category fits with more accuracy. The Van Krevelen chart is plotted (Fig. 4) and feces are located inside the biomass region, with atomic H:C ratio of 1.51 and O:C ratio of 0.80, closer to values from pine sawdust [1], sewage sludge [31] and peanut shell [32].

3.2 Products of gasification

3.2.1 Syngas analysis

During the gasification process, the composition of the permanent gases was established. Since the amount of the syngas composition is process dependent, the values presented here must be taken as estimated for the three moisture values. The species O_2, CO, H_2, NO and NOx were analyzed using electrochemical sensors, CO_2 levels were set using NDIR analyzer, and CxHy analysis used heated bead sensors. The results are expressed in vol. %.

Traces of NO and NOx were found, reaching maximum values of 100 ppm, regardless of the moisture levels. The total hydrocarbons CxHy were measured, but due to safety limitations of the device, it was not possible to conduct a

Table 2 Proximate and ultimate analysis and ash composition (wt%) of sterilized human feces and other solid residues from the literature

Proximate analysis	Moisture	Volatile matter	Fixed carbon	Ash
Human feces (this work)	17.30	50.20	25.10	7.40
Human feces, db [13]	–	82.00	0.00	18.00
Sugarcane bagasse [2]	8.30	72.00	10.60	9.10
Coconut shell [50]	10.10	75.5	11.20	3.20
Rice rusk [51]	8.54	65.45	15.60	10.41
Lignite [52]	12.00	42.00	31.00	15.00
Tobacco stem [53]	9.44	75.25	2.70	12.61
Coffee waste, db [54]	–	76.67	16.75	6.58
Wood, db [54]	–	85.58	14.34	0.08
Ultimate analysis	C	H	N	O
Human feces (this work)	49.07	7.41	4.50	39.02
Human feces, db [13]	48.15	6.92	5.21	21.64
Pine sawdust [1]	45.95	7.47	0.32	34.32
Sugarcane bagasse [2]	44.26	5.76	–	40.88
Sewage sludge 1 [31]	47.97	8.12	7.38	35.35
Sewage sludge 2 [55]	51.18	7.29	7.15	32.98
Tobacco seed [56]	44.20	6.96	6.85	42.00
Rice husk [51]	38.48	6.60	10.87	44.05
Peanut shell [32]	49.60	6.50	1.80	42.10
Banana leaves [57]	43.50	6.30	1.30	48.70
Tobacco stem [53]	38.02	6.20	2.73	51.93
Coffee waste [54]	51.33	6.79	3.02	31.60
Ash compositions	P_2O_5	CaO	K_2O	MgO
Human feces (this work)	47.64	21.63	17.51	10.30
Sewage sludge [31]	5.30	1.92	0.83	–
Forest residue [37]	11.60	28.60	23.90	6.70
Wood waste [36]	0.50	15.50	4.70	4.90

db dry basis

Table 3 Average volume fractions of the syngas components (% wb)

Moisture (%)	Species	Average composition (%)	σ_{avg} (%)	CI[a] (%)
0	CO	9.65	2.5	± 3.25
	H_2	6.56	0.6	± 0.35
	CO_2	6.54	0.4	± 0.44
	O_2	3.39	0.3	± 0.45
10	CO	8.11	0.25	± 0.17
	H_2	6.50	0.18	± 0.70
	CO_2	7.60	0.55	± 1.09
	O_2	2.03	0.18	± 0.79
20	CO	7.89	1.45	± 0.23
	H_2	3.91	0.62	± 1.00
	CO_2	6.23	0.45	± 0.50
	O_2	1.86	0.48	± 1.09

[a] Confidence interval of 95%

continuous measurement. Nevertheless, independent of the moisture content, all samples reached at least 4% at the beginning of the gasification process. The actual concentration of hydrocarbons will be calculated further by a mass balance (Sect. 3.3.1).

Figure 5 presents only the permanent measurements of O_2, CO_2, CO and H_2, together with the syngas temperature at the exit. The average molar fractions of the syngas components were calculated by integrating the curves in time intervals of: 704s to 2112s for 0% moisture, 670s to 2010s for 10% and 588s to 1764s for 20%. Note that these intervals are considered to be in the steady gasification since the temperature and O_2 reached a plateau and the gas flaring was active.

The average composition of H_2 decreased with the increase in moisture, from 6.56 to 3.91%, with low experimental uncertainty (0.62% average), while CO average composition slightly decreased, from 9.65 to 7.89%. However, the measurements uncertainties were higher for samples with 20% of moisture (6% maximum). CO_2 composition was relatively unaffected by the moisture content, staying in the range of 6.23–7.60%, with very low uncertainties (0.45% average). Finally, O_2 decreased from 3.39 to 1.86% with average uncertainty of 0.48%. The temperature decreased with the increase in moisture, from 833 to 786 °C, with average standard deviation of 33 °C. Table 3 summarizes the information above.

Returning to the analysis of Fig. 5, focusing on the classical chemical reactions involving $C_{(s)}$, CO, CO_2, H_2 and CxHy in gasification [33–36], the rate of formation and consumption of species provide inference on the pathway of syngas production. For example, the formation of CO and H_2 is distributed along the whole process for moisture contents of 0% and 10%, while for 20% the massive formation of the same species takes place at the beginning (300s to 800s). Also, since CO_2 curves follow the same fashion regardless of the moisture content, it suggests that the water-gas shift reaction ($CO + H_2O \leftrightarrow CO_2 + H_2$) contributes significantly to the CO_2 and H_2 formation; however, H_2 is consumed in another reaction, leading to the formation of hydrocarbon.

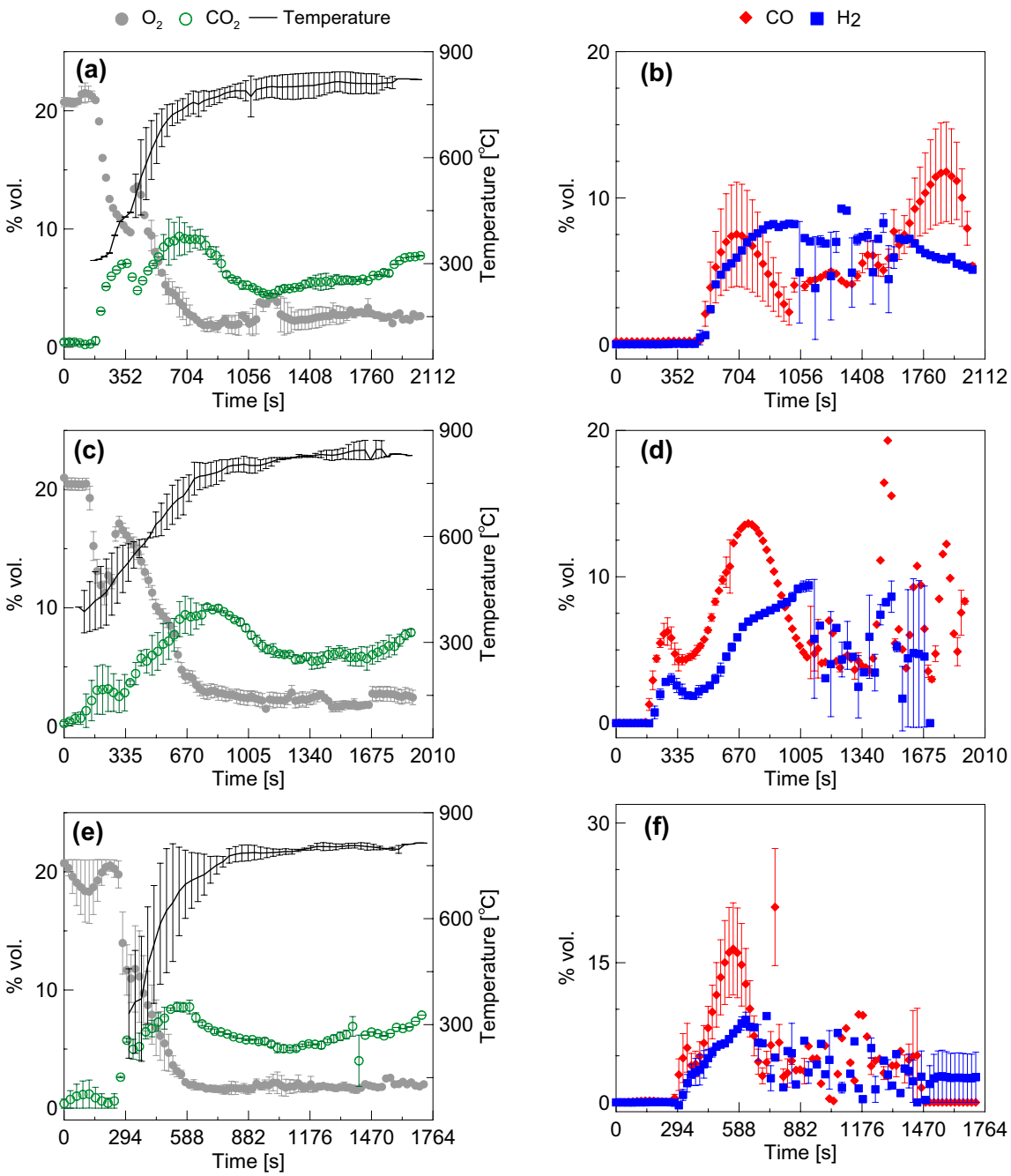

Fig. 5 Evolution of average temperature and gases formed during the batch gasification of sterilized human feces of varying moisture content: 0% (**a**, **b**), 10% (**c**, **d**) and 20% (**e**, **f**)

3.2.2 Ash composition

The ash formed had a sandy and whitish appearance, representing 7.4% of the feedstock initial mass. Although the ash had a sandy aspect, it easily turned into dust with simple hand friction. A small amount of sludge, around 8% of the ash mass, was also noted. It had harder consistency when compared to the ash. Table 2 shows the results for the main chemical components found in ash from feces and compares it with the ash from sewage sludge [31], forest residues [37] and wood waste [36], highlighting significant differences to the compounds formed.

Due to great levels of P, K, Ca and Mg, the ash generated from human feces gasification can be used as a fertilizer.

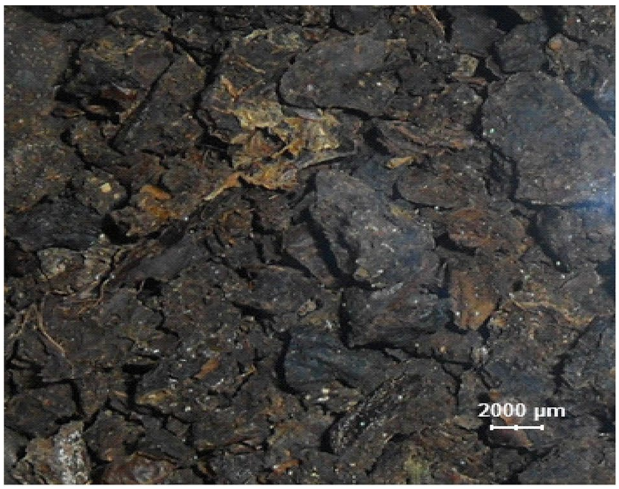

(a) Human feces after sterilization.

(b) Ash from human feces gasification.

Fig. 6 Transformation of human feces after sterilization to ash with sandish and white appearance, formed after the gasification process

Another possible destination for the product is the construction industry, where the ash may be used to produce magnesium potassium phosphate cements (MKPCs) [38], since great levels of MgO are observed. Oxides like Al_2O_3, SO_2, Fe_2O_3, MnO, CuO, SiO_2, B_2O_3, PbO, CdO and HgO completed the composition, representing around 3%.

The clean appearance and the lack of odor from the ash were characteristics observed that reinforced the sanitation contribution of the gasification process. Figure 6 shows the before (raw human feces) and after (ash) gasification.

3.3 Thermodynamic analysis

3.3.1 Mass balance

To perform a mass balance, Eq. 1 is taken into account for 1 kg of human feces. The stoichiometric coefficients are obtained from the proximate and ultimate analyses of the sample. Also, in the syngas, there is a small molar fraction of NO and NOx, which is neglected in the analysis. The chemical reaction is also written considering 10% and 20% of moisture, Eqs. 2 and 3, respectively.

$$\begin{aligned}&(40.85\,C + 73.51\,H + 24.39\,O^{+}3.21\,N + 0\,H_2O + ASH)\\&+12.75\,(O_2 + 3.76\,N_2) + 1.58\,H_2O \rightarrow 10.43\,CO\\&+7.09\,H_2 + 10.7\,C_{2.18}H_{2.18} + 7.07\,CO_2 + 19.57\,H_2O\\&+ 49.57\,N_2 + 3.66\,O_2 + ASH\end{aligned} \quad (1)$$

$$\begin{aligned}&(36.77\,C + 66.16\,H + 21.95\,O + 2.89\,N + 5.55\,H_2O + ASH)\\&+ 9.93\,(O_2 + 3.76\,N_2) + + 1.23\,H_2O \rightarrow 7.65\,CO\\&+ 6.13\,H_2 + 9.95\,C_{2.21}H_{2.21} + 7.17\,CO_2 + 22.76\,H_2O\\&+ + 38.79\,N_2 + 1.92\,O_2 + ASH\end{aligned} \quad (2)$$

$$\begin{aligned}&(32.68\,C + 58.81\,H + 19.51\,O + 2.57\,N + 11.10\,H_2O + ASH)\\&+ 9.20\,(O_2 + 3.76\,N_2) + 1.14\,H_2O \rightarrow 7.20\,CO\\&+ 3.57\,H_2 + 9.04\,C_{2.19}H_{2.19} + 5.69\,CO_2 + 28.18\,H_2O\\&+ + 35.89\,N_2 + 1.70\,O_2 + ASH\end{aligned} \quad (3)$$

The stoichiometric coefficients of the air components and the remaining syngas components are obtained in molar basis by the atomic balance of C, H, O and N. Besides, it is used the psychrometric definition of relative humidity and the definition of air–fuel ratio. To account the total mass of air which enters the gasifier, the batch process interval is considered along with the properties of humid air, obtained from the EES Air H_2O package.

From Eqs. 1, 2 and 3, it is noted that the respective H/C ratios for the syngas hydrocarbons are approximately equal to 1. Since one knows that light hydrocarbons are yielded from gasification processes, it is considered that the hydrocarbons behave as an average hydrocarbon modeled as acetylene, C_2H_2. Table 3 shows the average molar fractions of the syngas components in wet basis. Note that, regardless of the moisture content, H_2/CO, CO_2/CO and CxHy/CO ratios are around 0.7, 0.8 and 1.2, respectively.

The equivalent ratio (ER) parameter indicates whether a fuel–oxidizer mixture is rich, lean or stoichiometric [39]. The calculation takes into account the air–fuel ratio for the

complete combustion of the fecal materials (0%, 10% and 20% of moisture) and the theoretical amount of dry air (Eqs. 4, 5 and 6).

$$(40.85\,C + 73.51\,H + 24.39\,O + 3.21\,N + 0\,H_2O + ASH) + 47.04\,(O_2 + 3.76\,N_2) \rightarrow 40.85\,CO_2 + 36.76\,H_2O + 178.56\,N_2 + ASH \quad (4)$$

$$(36.77\,C + 66.16\,H + 21.95\,O + 2.98\,N + 5.55\,H_2O + ASH) + 42.33\,(O_2 + 3.76\,N_2) \rightarrow 36.77\,CO_2 + 38.63\,H_2O + 160.70\,N_2 + ASH \quad (5)$$

$$(32.68\,C + 58.81\,H + 19.51\,O + 2.57\,N + 11.10\,H_2O + ASH) + 37.63\,(O_2 + 3.76\,N_2) \rightarrow 32.68\,CO_2 + 40.51\,H_2O + 142.85\,N_2 + ASH \quad (6)$$

Finally, to obtain the syngas mass (m_{syn}), the mass balance equation (Eq. 7) is applied considering the mass of the feces from the batch process (m_{fuel}), the mass of ash recovered at the end of the experiment (m_{ash}) and the mass of air (m_{air}) measured at the inlet.

$$m_{fuel} + m_{air} = m_{ash} + m_{syn} \quad (7)$$

3.3.2 Energy balance

Figure 7 shows the molar composition (y_i) and the temperature of the syngas (T_{syn}) for each moisture content, which are going to be used in the energy balance. The ash temperature (T_{ash}) used in the model is the same as the syngas temperature, and it is treated as sand, modeled as an incompressible substance, with specific heat capacity ($c_{p,ash}$) obtained from [40].

The lower heating value of the raw material (LHV_{fuel}) in wet basis is obtained from its higher heating value (HHV_{fuel}) in dry basis, proximate analysis and ultimate analysis (Table 2). Equation 8 is applied, where W is the moisture mass fraction and X is the hydrogen mass fraction in wet basis.

$$LHV_{fuel} = (1 - W)(HHV_{fuel} - 9 \cdot X \cdot 2440) - (W \cdot 2440) \quad (8)$$

Regarding the energy entering and leaving the control volume, it is necessary to make some considerations: The air enters the gasifier at the standard reference temperature, $T_{ref} = 25\,°C$; the syngas is modeled as an ideal gas mixture; specific enthalpies (h_i) and molar masses (M_i) of each syngas component i are retrieved from the EES Ideal Gases package. With that stated, the energy that enters the gasifier with the feedstock (H_{fuel}) is given by Eq. 9. The energy that exits with syngas (H_{syn}) and ash (H_{ash}) is given by Eqs. 10 and 11, respectively. The energy balance of the process is given by Eq. 12, also considering the heat losses through the walls (Q_L).

$$H_{fuel} = m_{fuel} \cdot LHV_{fuel} \quad (9)$$

$$H_{syn} = \frac{m_{syn}}{\sum y_i \cdot M_i} \cdot \sum y_i \cdot M_i \cdot [h_i(T_{syn}) - h_i(T_{ref})] \quad (10)$$

$$H_{ash} = m_{ash} \cdot c_{p,ash} \cdot (T_{ash} - T_{ref}) \quad (11)$$

$$H_{fuel} = H_{syn} + H_{ash} + Q_L \quad (12)$$

Therefore, the main performance indicator of gasifiers is computed by the cold gas efficiency (Eq. 13), which takes into account the lower heating value of the syngas (LHV_{syn}), given by Eq. 14, and the lower heating value of the fuel, calculated previously.

$$CGE = \frac{LHV_{syn}}{LHV_{fuel}} \quad (13)$$

$$LHV_{syn} = \frac{\sum y_i \cdot M_i \cdot LHV_i}{\sum y_i \cdot M_i} \quad (14)$$

3.3.3 Exergy balance

The exergy analysis was carried out to determine the source, location and magnitude of inefficiencies related to the gasification process. Equation 15 gives the specific chemical exergy for a solid fuel (b^{CH}_{fuel}), where the term ϕ_{dry} is calculated from Eq. 16. The mass fractions ratios H/C, N/C and O/C are on wet basis.

$$b^{CH}_{fuel} = (LHV_{fuel} + 2442\,W) \cdot \phi_{dry} \quad (15)$$

$$\phi_{dry} = \frac{1.0438 + 0.1882(H/C) - 0.2509(1 + 0.7256H/C) + 0.0383(N/C)}{1 - 0.3035(O/C)} \quad (16)$$

The specific physical exergy of the syngas (b^{PH}_{syn}) is given by Eq. 17, considering, for the sake of simplicity, an average specific heat capacity of the syngas, $c_{p,syn}$ (Eq. 18). Equation 19 gives the specific chemical exergy of the syngas (b^{CH}_{syn}). The standard specific molar chemical exergy of each syngas component ($\bar{b}^{CH,0}_i$) was taken from [25].

$$b^{PH}_{syn} = c_{p,syn} \cdot (T_{syn} - T_0) - T_0 \cdot c_{p,syn} \cdot ln\frac{T_{syn}}{T_0} \quad (17)$$

$$c_{p,syn} = \frac{H_{syn}}{m_{syn} \cdot (T_{syn} - T_0)} \quad (18)$$

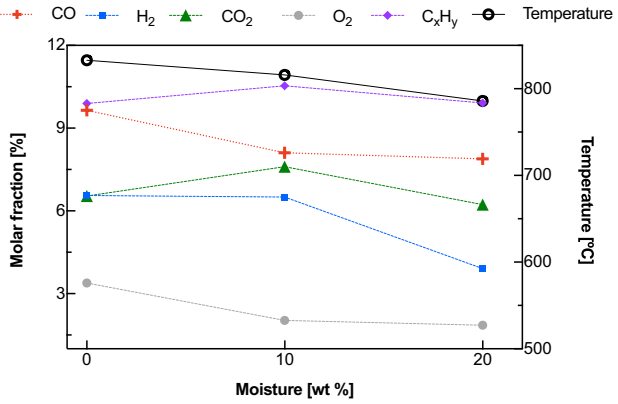

Fig. 7 Temperature and molar composition of the syngas produced by batch gasification of human feces samples with 0, 10 and 20% of moisture

$$b_{syn}^{CH} = \frac{\sum_i y_i \cdot \bar{b}_i^{CH,0} + \bar{R}.T_0 \cdot \sum_i y_i \cdot lny_i}{\sum_i y_i \cdot M_i} \quad (19)$$

To obtain the irreversibility of the gasification process, the exergy balance equation is applied (Eq. 20). The total irreversibility (I_{cv}) is the sum of the exergy destruction, due to the entropy generation, and the exergy loss associated with the ashes and the stray heat transfer.

Table 4 Calculation results from the exergy analysis, for samples with 0, 10 and 20% of moisture

Variable (unit)	0%	10%	20%
ER	0.2755	0.2383	0.2484
m_{air}(kg)	0.534	0.4157	0.3853
m_{ash}(kg)	0.0222	0.0200	0.0178
m_{syn}(kg)	0.8118	0.6957	0.6675
N_2 (%)	45.86	41.10	39.33
H_2O(%)	18.10	24.12	30.88
LHV_{fuel}(kJ/kg)	21,573	19,171	16,770
H_{fuel}(kJ)	6472	5751	5031
H_{ash}(kJ)	15	13	11
H_{syn}(kJ)	931	811	753
Q_L(kJ)	5526	4928	4267
LHV_{syn}(kJ/kg)	6575	6846	6307
CGE (%)	30.48	35.71	37.61
ϕ_{dry}	1.051	1.051	1.051
b_{fuel}^{CH}(kJ/kg)	22,673	20,406	18,139
cp_{syn}(kJ/kg)	1.42	1.47	1.48
b_{syn}^{PH}(kJ/kg)	592	596	568
b_{syn}^{CH}(kJ/kg)	6584	6896	6385
I_{CV}(kJ)	976	909	800
ε_{cold}(%)	78.58	78.38	78.33
ε_{hot}(%)	85.65	85.15	85.29

$$I_{cv} = m_{fuel} \cdot b_{fuel}^{CH} - m_{syn} \cdot (b_{syn}^{PH} + b_{syn}^{CH}) \quad (20)$$

Another two exergy-based indexes are used herein. The first one is the cold gas exergetic efficiency, ε_{cold} (Eq. 21), which takes into account the syngas chemical exergy only. The other one is the hot gas exergetic efficiency, ε_{hot} (Eq. 22), which takes into account both physical and chemical exergy of the syngas.

$$\varepsilon_{cold} = \frac{m_{syn} \cdot b_{syn}^{CH}}{m_{fuel} \cdot b_{fuel}^{CH}} \quad (21)$$

$$\varepsilon_{hot} = \frac{m_{syn} \cdot (b_{syn}^{PH} + b_{syn}^{CH})}{m_{fuel} \cdot b_{fuel}^{CH}} \quad (22)$$

Table 4 summarizes the calculation results from the whole thermodynamic analysis, considering the 0%, 10% and 20% moisture for human feces samples. While quantifying experimentally the heat losses during the gasification process, it was found a large amount of energy leaving the system, around 85%, regardless of the moisture content. For this reason, it is not desirable to establish a comparison with works developed under the assumptions of the adiabatic reactor and equilibrium modeling [12, 19, 41–43]. These assumptions lead to an inaccurate syngas yield, since the temperature levels become much higher than reality and sometimes unreal, carrying the Gibbs minimization process to overestimate CO and H_2 and underestimate or even neglect CxHy concentration. Specifically for low-rank solid fuels, the ratio LHV_{syn}/LHV_{fuel} is unrealistic, because LHV_{syn} is overestimated.

Regarding the irreversibilities (I_{CV}), it is noted that it decreases with the increase in moisture content. The explanation lies in the amount of O_2 that exits with the syngas (more than 3%, for 0% of moisture content—Fig. 7). The volatile compounds are responsible for adding O_2 radicals during the process, leading to local oxidation reactions inside the pyrolysis zone, as suggested by the exothermic behavior of pyrolysis. The main drawback of O_2 radicals released is to reduce the syngas quality and increase the exergy destruction. In this case, there is a direct relationship between the O_2 concentration and the ER. Zainal et al. [23] showed that by increasing the ER (from 0.25 to 0.37), the O_2 composition in the syngas is reduced (from 4.2 to 1.9 vol.%). Even so, when looking out the wood-dominant literature, e.g., refuse-derived fuel gasification, the opposite trend is observed [44].

Figure 8 displays the evaluation in terms of the physical and chemical exergy and the associated irreversibility, normalized by kg of fuel. Noteworthy, to the best of the

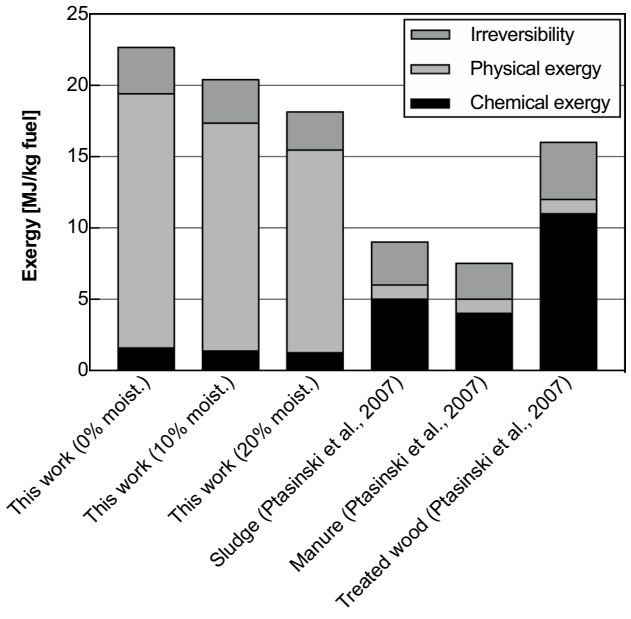

Fig. 8 Comparison between chemical exergy, physical exergy and irreversibility from batch gasification process of human feces and other solid fuels

authors, only [19] conducted a rigorous exergy analysis providing the data for comparison. While the irreversibility levels are close to other solid fuels, the physical exergy is higher than the chemical exergy, expressing the potential of energy that can be recovered from the streams of syngas, ash and walls. On the other hand, the chemical exergy is lower because the exergy destruction is accentuated due to unexpected chemical reactions, such as homogeneous/heterogeneous oxidations in the pyrolysis zone.

Despite the low-rank syngas produced, LHV_{syn} around 6.5 MJ/kg of fuel and CGE in the range of 30–38% (Table 4), it is still possible to use it in internal combustion engines due to favorable ratios of H_2/CO, CO_2/CO and CxHy/CO [45] and due to the high exergy efficiency (around 85%), which carries into calculation the ratio of m_{syn} and m_{fuel}. The solid and clean product is a thoroughly sanitized material that brings a negligible energetic impact on the process and great chemical exergy if used as a feedstock for a secondary process.

4 Conclusion and future perspective

The gasification of human feces showed some peculiarities along the whole process, from the raw material, with a strong odor and dark coloration, to an inert and cleaned material at the end. Yet, before a wide discussion, it is important to have a critical eye about some assumptions used in the literature to establish a fair comparison between the ideal and experimental-based gasification modeling.

A series of thermochemical characterization, from the raw material to the products of gasification, allowed to establish a factual thermodynamic assessment of the whole gasification process.

Regardless of the heterogeneous characteristics of the material, the average proximate analysis showed around 25% of fixed carbon and 50% of volatile matter. Part of this volatile matter, released at temperatures around 150 °C, could be associated with the exothermic characteristic of feces pyrolysis. The ash composition showed that some important minerals are trapped in the form of oxide, conferring a valuable asset to the material. Unlike the equilibrium models, which boost CO and H_2 composition, the online gas analysis revealed that CO, H_2, CxHy are effectively present, despite the low-rank syngas produced.

The outcome of this study is the critical relationship of moisture content of the feedstock and air, and the energy loss of the gasification process. The interplay suggests an unfavorable application in terms of energetic efficiency, varying from 30% (dry feces) to 38% (20% moisture); however, when the environmental bias is added together with the exergy analysis (exergy efficiency around 85%, regardless of the moisture content), the process becomes more attractive due to the potential of energy recovery and the possible use of small-scale gasifiers as a sanitation tool for materials with the moisture content up to the limitation of the device.

Looking into the future, many research efforts can be done to address the gasification of fecal excreta. Two main challenges arise from the present work and must receive considerable attention in the years to come:

- The concept of using gasification as on-site thermal technology combined with pit latrines and dry toilets. In low- and middle-income countries, the collection of human feces can be pointed as one of the most complex waste management problems. Therefore, the tanks of pit latrines and dry toilets [46], commons in these countries, must be part of the same system. The application seems favorable to the dry toilets since it separates the urine from feces.
- The direct conversion of raw human feces using existent thermal technologies. Even though the high physical exergy of the process shows a possibility to bring the moisture content to acceptable levels [23, 39, 47, 48], the direct conversion dealing with high water content is still a challenge. In this context, the concept of waste heat recovery must be addressed [49].

Compliance with ethical standards

Conflict of interest The author(s) declare that they have no competing interests.

References

1. Braz CEM, Crnkovic PCGM (2014) Physical–chemical characterization of biomass samples for application iin pyrolysis process. Chem Eng Trans 37:523–528
2. Kandasamy J, Gokalp I, Petrus S, Belandria V, Bostyn S (2018) Energy recovery analysis from sugar cane bagasse pyrolysis and gasification using thermogravimetry, mass spectrometry and kinetic models. J Anal Appl Pyrol. https://doi.org/10.1016/j.jaap.2018.02.003
3. Molino A, Chianese S, Musmarra D (2016) Biomass gasification technology: the state of the art overview. J Energy Chem 25(1):10. https://doi.org/10.1016/j.jechem.2015.11.005
4. Sansaniwal S, Rosen M, Tyagi S (2017) Global challenges in the sustainable development of biomass gasification: an overview. Renew Sustain Energy Rev 80:23. https://doi.org/10.1016/j.rser.2017.05.215
5. Rashwan TL, Gerhard JI, Grant GP (2016) Application of self-sustaining smouldering combustion for the destruction of wastewater biosolids. Waste Manag 50:201
6. Onabanjo T, Kolios AJ, Patchigolla K, Wagland ST, Fidalgo B, Jurado N, Hanak DP, Manovic V, Parker A, McAdam E et al (2016) An experimental investigation of the combustion performance of human faeces. Fuel 184:780
7. Yermán L, Hadden RM, Carrascal J, Fabris I, Cormier D, Torero JL, Gerhard JI, Krajcovic M, Pironi P, Cheng YL (2015) Smouldering combustion as a treatment technology for faeces: exploring the parameter space. Fuel 147:108. https://doi.org/10.1016/j.fuel.2015.01.055
8. Monhol F, Martins M (2015) Cocurrent combustion of human feces and polyethylene waste. Waste Biomass Valorization 6(3):425
9. Fabris I, Cormier D, Gerhard JI, Bartczak T, Kortschot M, Torero JL, Cheng YL (2017) Continuous, self-sustaining smouldering destruction of simulated faeces. Fuel 190:58
10. Yermán L, Wall H, Torero JL, Gerhard JI, Fabris I, Cormier D, Cheng YL, et al. (Engineers Australia, 2015) Self-sustaining smouldering combustion of faeces as treatment and disinfection method. In: Asia pacific confederation of chemical engineering congress 2015: APCChE 2015, incorporating CHEMECA 2015, p. 2677
11. Yermán L, Cormier D, Fabris I, Carrascal J, Torero J, Gerhard J, Cheng YL (2017) Potential bio-oil production from smouldering combustion of faeces. Waste Biomass Valorization 8(2):329
12. Onabanjo T, Patchigolla K, Wagland ST, Fidalgo B, Kolios A, McAdam E, Parker A, Williams L, Tyrrel S, Cartmell E (2016) Energy recovery from human faeces via gasification: a thermodynamic equilibrium modelling approach. Energy Convers Manag 118:364
13. Jurado N, Somorin T, Kolios AJ, Wagland S, Patchigolla K, Fidalgo B, Parker A, McAdam E, Williams L, Tyrrel S (2018) Design and commissioning of a multi-mode prototype for thermochemical conversion of human faeces. Energy Convers Manag 163:507
14. Yacob TW, Linden KG, Weimer AW et al (2018) Pyrolysis of human feces: gas yield analysis and kinetic modeling. Waste Manag 79:214
15. Roberts A (1971) The heat of reaction during the pyrolysis of wood. Combust Flame 17(1):79. https://doi.org/10.1016/S0010-2180(71)80141-4
16. Yang H, Yan R, Chen H, Lee DH, Zheng C (2007) Characteristics of hemicellulose, cellulose and lignin pyrolysis. Fuel 86(12—-13):1781
17. Bejan A (2002) Fundamentals of exergy analysis, entropy generation minimization, and the generation of flow architecture. Int J Energy Res 26(7):545–565
18. Kotas TJ (2013) The exergy method of thermal plant analysis. Elsevier, Amsterdam
19. Ptasinski KJ, Prins MJ, Pierik A (2007) Exergetic evaluation of biomass gasification. Energy 32(4):568
20. Pellegrini LF, de Oliveira JS (2007) Exergy analysis of sugarcane bagasse gasification. Energy 32(4):314
21. Gómez-Barea A, Leckner B (2010) Modeling of biomass gasification in fluidized bed. Prog Energy Combust Sci 36(4):444
22. Puig-Arnavat M, Bruno JC, Coronas A (2012) Modified thermodynamic equilibrium model for biomass gasification: a study of the influence of operating conditions. Energy Fuels 26(2):1385
23. Zainal Z, Rifau A, Quadir G, Seetharamu K (2002) Experimental investigation of a downdraft biomass gasifier. Biomass Bioenergy 23(4):283
24. APL (2016) Power Pallet 20 kW.http://wiki.gekgasifier.com/w/page/6123718/FrontPage. Accessed 12 Apr 2019
25. EES (2017) Engineering equation solver—EES. http://www.fchart.com. Accessed 12 Apr 2019
26. Garner CE, Smith S, de Lacy CB, White P, Spencer R, Probert CS, Ratcliffe NM (2007) Volatile organic compounds from feces and their potential for diagnosis of gastrointestinal disease. FASEB J 21(8):1675
27. Rossi M, Aggio R, Staudacher HM, Lomer MC, Lindsay JO, Irving P, Probert C, Whelan K (2018) Volatile organic compounds in feces associate with response to dietary intervention in patients with irritable bowel syndrome. Clin Gastroenterol Hepatol 16(3):385
28. Ohlemiller T (1985) Modeling of smoldering combustion propagation. Prog Energy Combust Sci 11(4):277. https://doi.org/10.1016/0360-1285(85)90004-8
29. Fatehi M, Kaviany M (1997) Modeling of smoldering combustion propagation. Int J Heat Mass Transf 40(11):2607. https://doi.org/10.1016/S0017-9310(96)00282-7
30. Somorin TO, Kolios AJ, Parker A, McAdam E, Williams L, Tyrrel S (2017) Faecal-wood biomass co-combustion and ash composition analysis. Fuel 203:781
31. Ko JH, Wang J, Xu Q (2018) Characterization of particulate matter formed during sewage sludge pyrolysis. Fuel 224:210. https://doi.org/10.1016/j.fuel.2018.02.189
32. Messina LG, Bonelli P, Cukierman A (2017) Effect of acid pretreatment and process temperature on characteristics and yields of pyrolysis products of peanut shells. Renew Energy 114:697
33. Susastriawan A, Saptoadi H (2017) Small-scale downdraft gasifiers for biomass gasification: a review. Renew Sustain Energy Rev 76(Supplement C):989
34. Mallick D, Mahanta P, Moholkar VS (2017) Co-gasification of coal and biomass blends: chemistry and engineering. Fuel 204:106. https://doi.org/10.1016/j.fuel.2017.05.006
35. Speight JG (2014) Chapter 2—Chemistry of gasification. In: J.G. Speight (ed) Gasification of unconventional feedstocks. Gulf Professional Publishing, Boston, pp. 30–53. https://doi.org/10.1016/B978-0-12-799911-1.00002-9
36. Zhang Y, Gao X, Li B, Zhang H, Qi B, Wu Y (2015) An expeditious methodology for estimating the exergy of woody biomass by means of heating values. Fuel 159:712
37. Zevenhoven-Onderwater M, Backman R, Skrifvars BJ, Hupa M (2001) The ash chemistry in fluidised bed gasification of biomass fuels. Part I: predicting the chemistry of melting ashes and ash-bed material interaction. Fuel 80(10):1489. https://doi.org/10.1016/S0016-2361(01)00026-6

38. Gardner LJ, Bernal SA, Walling SA, Corkhill CL, Provis JL, Hyatt NC (2015) Characterisation of magnesium potassium phosphate cements blended with fly ash and ground granulated blast furnace slag. Cem Concr Res 74:78. https://doi.org/10.1016/j.cemconres.2015.01.015
39. Jangsawang W, Laohalidanond K, Kerdsuwan S (2015) Optimum equivalence ratio of biomass gasification process based on thermodynamic equilibrium model. Energy Procedia 79:520
40. Zanoni MA, Torero JL, Gerhard JI (2017) Determination of the interfacial heat transfer coefficient between forced air and sand at Reynold's numbers relevant to smouldering combustion. Int J Heat Mass Transf 114:90
41. Janajreh I, Al Shrah M (2013) Numerical and experimental investigation of downdraft gasification of wood chips. Energy Convers Manag 65:783
42. Shabbar S, Janajreh I (2013) Thermodynamic equilibrium analysis of coal gasification using Gibbs energy minimization method. Energy Convers Manag 65:755
43. Mhilu CF (2012) Modeling performance of high-temperature biomass gasification process. ISRN Chem Eng 2012:437186. https://doi.org/10.5402/2012/437186
44. Khosasaeng T, Suntivarakorn R (2017) Effect of equivalence ratio on an efficiency of single throat downdraft gasifier using RDF from municipal solid waste. Energy Procedia 138:784
45. Wieckert C, Obrist A, Pv Z, Maag G, Steinfeld A (2013) Syngas production by thermochemical gasification of carbonaceous waste materials in a 150 kWth packed-bed solar reactor. Energy Fuels 27(8):4770
46. Strauss M, Barreiro W, Steiner M, Mensah A, Jeuland M, Bolomey S, Montangero A, Koné D (2006) Urban excreta management Situation, challenges, and promising solutions. In: Proceedings of the 1st international faecal sludge management policy symposium and workshop. Dakar, Senegal, pp. 9–12
47. Bermudez J, Fidalgo B (2016) 15—Production of bio-syngas and bio-hydrogen via gasification. In: Luque R, Lin CSK, Wilson K, Clark J (eds) Handbook of biofuels production, 2nd edn. Woodhead Publishing, Sawston, pp 431–494. https://doi.org/10.1016/B978-0-08-100455-5.00015-1
48. Svoboda K, Martinec J, Pohořelý M, Baxter D (2009) Integration of biomass drying with combustion/gasification technologies and minimization of emissions of organic compounds. Chem Papers 63(1):15. https://doi.org/10.2478/s11696-008-0080-5
49. Tańczuk M, Kostowski W, Karaś M (2016) Applying waste heat recovery system in a sewage sludge dryer—a technical and economic optimization. Energy Convers Manag 125:121
50. Rout T, Pradhan D, Singh R, Kumari N (2016) Exhaustive study of products obtained from coconut shell pyrolysis. J Environ Chem Eng 4(3):3696
51. Hossain M, Islam M, Rahman M, Kader M, Haniu H (2017) Biofuel from co-pyrolysis of solid tire waste and rice husk. Energy Procedia 110:453
52. Patel VR, Patel D, Varia N, Patel RN (2017) Co-gasification of lignite and waste wood in a pilot-scale (10Â kWe) downdraft gasifier. Energy 119:834. https://doi.org/10.1016/j.energy.2016.11.057
53. Chen Z, Leng E, Zhang Y, Zheng A, Peng Y, Gong X, Huang Y, Qiao Y (2018) Pyrolysis characteristics of tobacco stem after different solvent leaching treatments. J Anal Appl Pyrol 130:350. https://doi.org/10.1016/j.jaap.2017.12.009
54. Skreiberg A, Skreiberg O, Sandquist J, Sorum L (2011) TGA and macro-TGA characterisation of biomass fuels and fuel mixtures. Fuel 90(6):2182. https://doi.org/10.1016/j.fuel.2011.02.012
55. Syed-Hassan SSA, Wang Y, Hu S, Su S, Xiang J (2017) Thermochemical processing of sewage sludge to energy and fuel: fundamentals, challenges and considerations. Renew Sustain Energy Rev 80:888
56. Onorevoli B, da Silva Maciel GP, Machado ME, Corbelini V, Caramão EB, Jacques RA (2018) Characterization of feedstock and biochar from energetic tobacco seed waste pyrolysis and potential application of biochar as an adsorbent. J Environ Chem Eng 6:1279–1287
57. Fernandes ERK, Marangoni C, Souza O, Sellin N (2013) Thermochemical characterization of banana leaves as a potential energy source. Energy Convers Manag 75:603